

1 WF17033

2 E. Pastor *et al.*

3 Smouldering field experiments

4 **A new method for performing smouldering combustion field experiments in**
5 **peatlands and rich-organic soils**

6 E. Pastor^{A,F}, I. Oliveras^B, E. Urquiaga-Flores^C, J. A. Quintano-Loayza^D, M. I. Manta^E and E.
7 Planas^A

8 ^ADepartment of Chemical Engineering, Centre for Technological Risk Studies, Universitat
9 Politècnica de Catalunya·BarcelonaTech, Eduard Maristany 10-14, E-08019 Barcelona,
10 Catalonia, Spain.

11 ^BEnvironmental Change Institute, School of Geography and the Environment, University of
12 Oxford, South Parks Road, Oxford OX13QY, UK.

13 ^CDepartment of Systematic and Evolutionary Botany, University of Zurich, Zollikerstrasse
14 107, CH-8088 Zurich, Switzerland.

15 ^DDepartment of Botany, Universidad de San Antonio Abad del Cusco, Avenida Cultura 733,
16 Cusco, Perú.

17 ^EForest Management Department, Universidad Nacional Agraria La Molina, Avenida La
18 Universidad S/N, , Apartado 12-056, Lima, Perú.

19 ^FCorresponding author. Email: elsa.pastor@upc.edu

20 Smouldering ground fires have severe environmental implications. Their main effects are the release of
21 large amounts of carbon to the atmosphere with losses of organic soil and its biota. Quantitative data on
22 the behaviour of smouldering wildfires are very scarce and are needed to understand its ecological effects,
23 to validate fuel consumption and smouldering propagation models and to develop danger-rating systems.
24 We present, for the first time, a methodology for conducting smouldering experiments in field conditions.
25 This method provides key data to investigate smouldering combustion dynamics, acquire fire behaviour
26 metrics and obtain indicators for ecological effects of smouldering fires. It is to be applied in all types of
27 undisturbed soils. The experimental protocol is based on a non-electric ignition source and the monitoring
28 system relies on combining both point and surface specific temperature measurements. The methodology
29 has been developed and applied by means of large series of replicate experiments in highly organic soils
30 at the forest–grassland treeline of the Peruvian Andes. The soil tested exhibited weak ignition conditions.
31 However, transition to oxidation phase was observed, with smouldering combustion during 9 h at 15-cm
32 depth and residence times at temperatures above dehydration of ~22 h.

33 **Additional keywords:** carbon emission, charcoal combustion, ground fires, infrared imagery,
34 Peruvian Andes, thermal damage.

35 We present a method for conducting smouldering experiments in field conditions by which data on fire
36 behaviour and ecological effects of ground fires are obtained at real scale. The methodology is tested at
37 the forest–grassland treeline of the Peruvian Andes. We observe smouldering during 9 h at 15-cm depth.

38 **Introduction**

39 Peatlands are a key component of the global carbon pool. They cover only 2–3% of the
40 global terrestrial surface but store over 25% of the world’s soil carbon (Yu 2012). Despite their
41 importance, peatlands are being rapidly depleted because of land use changes (e.g. drainage for
42 oil palm plantation in Indonesia and Malaysia, Moore *et al.* 2013) and fires (Page *et al.* 2002;
43 Turetsky *et al.* 2014). Peat fires are characterised by smouldering combustion, a slow, flameless
44 and low-temperature combustion of the organic matter in porous form (Ohlemiller 1985; Rein
45 2009). The controlling mechanisms of soil smouldering fires are still scarcely known (Rein
46 2009), although there is plenty evidence of their daunting effects on certain ecosystems (Page *et al.*
47 *et al.* 2002; Rein 2009; Davies *et al.* 2013). Smouldering fires can persist for long periods (months
48 to years), totally consuming the soil and thus creating a devastated landscape. For example,
49 during October and November 2015, more than 10 000 forest fires destroyed large peatland
50 regions across Kalimantan (Indonesian Borneo) and Sumatra (Carrington 2015). These events
51 matched at least the fires of 1997, the worst year on record on peatland fires, which released
52 between 0.98 and 2.6 Gt of carbon to the atmosphere (Page *et al.* 2002). Temperate peatlands
53 are also increasingly being affected by smouldering fires even in managed systems like in the
54 UK (Davies *et al.* 2013), as well as are boreal systems – for example, it has been estimated that
55 Russian boreal forest fires accounted to 15–20% of the annual global carbon emissions from
56 forest fires in 1998 (Conard *et al.* 2002).

57 The most common triggering events of extensive smouldering combustion are wildfires,
58 either natural or, most frequently, human-induced. In tropical regions, fires from deforestation
59 and land clearing are usually the starting point for smouldering combustion, especially in El
60 Niño years (Page *et al.* 2009). In temperate regions, management prescribed burnings are often
61 the cause of these fires (Davies *et al.* 2016). The effects of ground fires are the release of very
62 large amounts of carbon to the atmosphere with the consequent losses of organic soil, complete
63 mortality of soil biota and all vegetation existing in that landscape.

64 Smouldering combustion in organic soils propagates laterally and downwards by an overall
65 exothermic process composed by three stages (Fig. 1). First, the smouldering front preheats
66 gradually the medium ahead at dehydration temperatures ~50–100°C (Filkov *et al.* 2012).

67 Once dehydrated, the dry medium experiences endothermic reactions of pyrolysis at
68 temperatures above 150°C (Phase 2) (Chen *et al.* 2011), in which the chemical breakdown of
69 the solid fuel yields char (carbon-enriched solid material), pyrolysate gases and ash. In
70 smouldering combustion, *in situ* char oxidation dominates gas-phase oxidation. Last (Phase 3),
71 char oxidation reactions take place once ignition temperatures (above 210°C) are reached
72 (Babrauskas 2003) and sufficient transfer of oxygen is guaranteed, giving heat, CO₂, CO and
73 water vapour as main combustion products.

74 The intensity and rate of spread of a smouldering subsurface wildfire front is primarily
75 controlled by the heat losses to the environment and by the oxygen transfer to the combustion
76 zone (Ohlemiller 1985). The soil properties that allow for a sustained smouldering ignition and
77 propagation are soil moisture, mineral content, bulk density, soil depth, porosity, permeability
78 and organic composition of the different subsurface layers involved (Rein 2009). Although it is
79 well known that all of these factors may play a certain role in the overall smouldering
80 combustion processes, the relative importance of each, their interaction and effects on
81 smouldering fire behaviour (e.g. spread rate, residence time, heat released, fuel consumption) in
82 different types of soils and ecosystems are still poorly understood (Rein 2013).

83 Smouldering evidences of real wildfires (e.g. depth of burn) have been quantified in the
84 literature (e.g. de Groot *et al.* 2009; Turetsky *et al.* 2011). However, quantitative data on the
85 actual behaviour of smouldering wildfires are very scarce (Usup *et al.* 2004), because the
86 stochastic and unforeseen nature of these events makes the development of systematic and
87 reliable sampling methodologies in real wildfire scenarios a very challenging task. Data on
88 smouldering fires related variables are needed to better understand its ecological effects and
89 positive feedbacks to climate change (Bertschi *et al.* 2003; Davies *et al.* 2013), and to validate
90 fuel consumption and smouldering propagation models (Grishin *et al.* 2009) and danger rating
91 systems (Reardon *et al.* 2009). However, despite the ideal environment to study smouldering
92 would be a field scenario (Frandsen 1987), smouldering field experiments have never been
93 reported in the peer-reviewed literature. To the best of our knowledge, there were some limited
94 attempts of ignition field tests in Engelman spruce duff in 1995 (Lawson *et al.* 1997), but those
95 authors did not report any combustion metrics nor a well described methodology.

96 Because of these challenges, smouldering combustion in ground fuels has so far only been
97 studied in laboratory conditions (or more recently, using computational models to recreate
98 laboratory set ups as in Huang *et al.* 2015). Most of these experiments have provided valuable
99 insights defining ignition and sustained combustion thresholds associated to soil moisture,
100 inorganic content, fuel depth and density. These studies have used different approaches to

101 induce combustion – the most common is an electrically heated coil (e.g. Frandsen 1987;
102 Miyanishi and Johnson 2002; Garlough and Keyes 2011), as well as different soil substrates –
103 whereas some have used commercial disaggregated peat-moss to emulate real natural fuels
104 (Frandsen 1987, 1998; Hartford 1989; Miyanishi and Johnson 2002; Prat *et al.* 2015), some
105 others have used field samples (Frandsen 1991, 1997; Reardon *et al.* 2007; Rein *et al.* 2008;
106 Benscoter *et al.* 2011; Garlough and Keyes 2011). All these studies have artificially varied some
107 of the sample properties to meet specific research objectives, being the most common
108 manipulations moisture (by moistening and/or drying samples – e.g. Garlough and Keyes 2011),
109 addition of inorganic substrate (inorganic content manipulation – e.g. Frandsen 1987) and/or
110 mechanical compaction (soil density manipulation – e.g. Miyanishi and Johnson 2002;
111 Garlough and Keyes 2011). Laboratory studies usually use punctual temperature measurements
112 to monitor combustion and fire behaviour (e.g. Rein *et al.* 2008; Benscoter *et al.* 2011) with
113 only few studies using continuous monitoring such as infrared (IR) imagery systems to extract
114 quantitative data (Prat-Guitart *et al.* 2015, 2016; Huang *et al.* 2016). These controlled laboratory
115 studies have provided a clear step forward on our current understanding of smouldering fire
116 behaviour. However, they barely replicate natural conditions. For example, the majority of
117 laboratory studies published so far have suggested that the ignition limit of organic soil horizons
118 is at moisture content (on wet base) of 150% or less (Garlough and Keyes 2011). However,
119 smouldering in peat wildfires has been reported to be sustained at higher moisture contents (e.g.
120 average values of 252 and 273% (dry base) found in Davies *et al.* 2013) and recent simulation
121 studies (250% dry base, Huang and Rein 2015; Thompson *et al.* 2015) and laboratory studies
122 (Watts 2013 also finds a 250% dry base moisture content threshold) also suggest so. In addition,
123 the inability of laboratory methods to reproduce real smouldering downward propagation
124 patterns has already been noted (Watts 2013).

125 Moisture is a key factor when determining whether smouldering combustion is sustained and
126 is highly influenced by inorganic content, soil density and soil depth (Frandsen 1987; Miyanishi
127 and Johnson 2002; Reardon *et al.* 2007; Garlough and Keyes 2011). In most laboratory
128 experiments, moisture content has been manipulated to be homogeneous within the samples.
129 However, natural ground fuel is heterogeneous, with moisture, inorganic content and soil
130 density varying laterally and vertically (e.g. Bridge and Johnson 2000; Zoltai *et al.* 2000;
131 Benscoter *et al.* 2005). Frandsen (1987) already highlighted the importance of natural moisture
132 gradients in controlling the ignition and propagation of smouldering fronts. In fact, assumptions
133 of homogeneity have already been considered invalid for thick organic soils (Benscoter *et al.*
134 2011) and some authors have already stressed that the validity of their results depends on real
135 moisture and mineral content distributions (Reardon *et al.* 2007; Garlough and Keyes 2011).

136 This study presents, for the first time, a novel methodology for conducting smouldering
137 experiments in field conditions. The methodology is envisaged to provide data to: (i) analyse the
138 transition of the several combustion stages at different depths and locations; (ii) extract
139 smouldering fire behaviour metrics; and (iii) obtain indicators for ecological effects of
140 smouldering fires. Our proposed methodology can potentially be applied to study any type of
141 subsurface organic layer and environment. It is particularly suitable for systems with difficult
142 properties for being replicated at laboratory scale (high density soils, colloidal soils, soils with
143 wide ranges on characteristic properties, etc.). The paper is organised as follows: we first
144 present the methodology rationale giving details on the main assumptions regarding the aim and
145 scope of the methodology, the experimental layout and the ignition source and smouldering
146 monitoring. Next, we provide extensive information on the methodology development and
147 testing through a study case conducted to investigate smouldering combustion on the humic
148 layers of high-latitude Andean grassland soils exposed to real weather conditions. We then
149 discuss the suitability of our method and the significance of the experimental results obtained in
150 our study case, by comparing our protocol with laboratory procedures, by presenting some
151 insights on how ground fires are sustained and by estimating the final fire behaviour and
152 ecological effects metrics regarding our experiments. Finally, we provide some concluding
153 remarks and outline further work.

154 **Methodology rationale**

155 An experimental method for studying smouldering combustion on field conditions requires a
156 careful design taking into account several aspects about its applicability and operability. The
157 underlying assumptions considered when developing the method are detailed as follows.

158 *Scope and objectives*

159 The final aim of the method is to provide quantitative data on smouldering fire behaviour
160 metrics and indicators under field conditions (e.g. rate of spread, smouldering transition
161 thresholds, fire residence time, carbon lost) to be mainly used for ecological effects analysis and
162 models validation (fuel consumption, fire propagation, danger rating, etc.). The methodology is
163 not foreseen to be used as a procedure to analyse the particular involvement of a certain soil
164 property on the smouldering ignition and propagation phenomena. Rather, the method is
165 intended to provide a detailed picture in terms of smouldering fire behaviour and related
166 parameters under realistic conditions. The methodology should be applicable and generalisable
167 to all sorts of smouldering-prone soils, regardless its eco-zone and location, respecting the
168 nature of the organic horizons, preserving soil natural variations and hence assuring a realistic
169 scenario.

170 *Experimental layout*

171 The protocol should take into account the natural soil heterogeneity, the eventually variable
172 weather conditions and should allow large series of experiments with multiple replications. For
173 this reason, it should consider a layout with different experimental blocks covering different
174 areas of the selected study site. Within each block, several plots should be designed to account
175 for true replicates (to be burnt at the same time) and for control plots (to monitor soil
176 properties). The number of blocks and plots should reflect a good compromise between results
177 significance and experimental program complexity and effort.

178 *Ignition source and smouldering monitoring*

179 The ignition procedure should be quantifiable, easy to replicate, realistic, independent of
180 external energy sources and easy to implement in isolated areas. The monitoring system should
181 have a positive trade-off between monitoring effort and quality/quantity of the data needed.
182 Ideally, it should contemplate a combination of point (thermocouples) and surface specific
183 (infrared imagery) temperature measurements. Thermocouples disposed in a spatial and soil-
184 depth array in the study area should provide the temperature–time evolution of the smouldering
185 front to analyse smouldering dynamics and compute fire behaviour and fire effects metrics.
186 Processing temperature–time curves should enable to obtain data on the smouldering transition
187 thresholds, on the rate of spread of the smouldering front and on the residence times of the heat
188 front at different temperatures (e.g. [Usup et al. 2004](#); [Rein et al. 2008](#)). Moreover, time-
189 integrated temperatures above certain temperature thresholds should provide an indicator of the
190 accumulated heat that the medium experiences over time, containing valuable information to
191 analyse fire severity and other ecological effects (e.g. [Kennard et al. 2005](#); [Bova and Dickinson
2008](#)). The optimum thermocouples layout should consider several sensors at different depths
193 (according to the soil moisture content profile) and should be evenly distributed through the
194 plots surface. In contrast, infrared imagery should allow surface temperature surveys at certain
195 periods, and should provide information about the overall area affected by combustion activity
196 (e.g. [Plucinski and Pastor 2013](#); [Prat-Guitart et al. 2015](#)). This type of data should be useful to
197 control the course of the experiments, to assess fuel consumption and, provided carbon content
198 is known, to estimate carbon lost during smouldering.

199 **Methodology development and testing: study case in Andean Puna organic soil**

200 *Experimental site*

201 The study was carried out in the high-altitude Andean grasslands of the south-eastern
202 Peruvian Andes ([Fig. 2](#)), at ~3300 m above sea level (ASL) in the south-western buffer area of
203 Manu National Park (13°10'50.28"S, 71°35'19.95"W). These grasslands are characterised by

204 tussock-forming grasses. Dominant species include *Calamagrostis longearistata*, *Ageratina*
205 *sternbergiana*, *Juncus bufonius* and *Scirpus rigidus* (Oliveras *et al.* 2014a). Average annual
206 rainfall ranges from 1900 to 2500 mm, with a wet season spanning from October to April. Mean
207 annual temperature were $\sim 11^{\circ}\text{C}$ at 3600 m ASL (Gibbon *et al.* 2010). Soils are composed of a
208 thick organic-rich A-layer, stony B/C-layers, and a thin or no Oh-layer (Zimmermann *et al.*
209 2010; Oliveras *et al.* 2014b). At the study site, the organic rich layer varied between 60 and
210 110 cm. One of the key aspects of fires in the region is the occurrence of smouldering (Román-
211 Cuesta *et al.* 2011; Oliveras *et al.* 2013) and we aimed to study the conditions that would enable
212 ignition and sustained combustion of the soil organic layers. The study was developed within
213 the framework of a larger project aimed at characterising the dynamics of forest fires at the
214 forest-grassland treeline of the Peruvian Andes (Oliveras *et al.* 2014a, 2014b, 2014c; Román-
215 Cuesta *et al.* 2014).

216 *Experimental design*

217 The experimental set up consisted of a randomised block design of two blocks, 500 m apart
218 located in a relatively flat area with no grazing, with 20 plots (0.5×0.5 m) each (see Fig. 2).
219 Plots dimensions were established according to typical smouldering front propagation values
220 (Rein (2009) provides typical front rate of spread values of $1-3 \text{ cm h}^{-1}$ meaning that a 50×50 -
221 cm plot should be burned between 16 h and 50 h hence ensuring a long monitoring period). At
222 each block (named W1 and W2), five plots were randomly selected as control plots (to be left
223 unburned and to control soil moisture content), and excepting on these, metal plates were
224 inserted in all plots up to 0.5 m soil deep in order to avoid any eventual smouldering front to
225 propagate out of the plot (in deeper regions, according to preliminary soil-moisture content
226 measurements and according to visual inspections, we assumed that the soil was too moist and
227 dense to sustain smouldering combustion). We initially set a planning consisting on five
228 experimental days, burning each day six plots (three at every block, randomly selected and
229 acting as true replicates), but bad meteorological conditions only allowed us to perform burns
230 on 3 days (Table 1). Therefore, burns were performed on eighteen plots on 7, 10 and 11 July
231 2012, starting between 1030 and 1430 hours local time. All experiments were left to burn for
232 48 h.

233 *Ignition procedure*

234 We established an ignition procedure that consisted on introducing 1 kg of smouldering
235 charcoal in a 30 cm long \times 10 cm wide \times 20 cm deep hole dug at one of the ends of the plot.
236 Charcoal was preliminary activated with a portable gas burner outside the plot. The hole had the

237 back side protected with firebricks against an eventual undesired spread direction, enabling our
238 design smouldering propagation forwards only (Fig. 3).

239 An estimate of the power supply of the ignition source was made based on charcoal burning
240 properties. Instantaneous charcoal burning rate (\dot{M}_i , kg s⁻¹) depends, according to D. Andreatta
241 (pers. comm., 30 May 2013), on the mass of charcoal remaining at each time instant i (M_{ri} , kg)
242 and can be approximated by the following equation:

243
$$\dot{M}_i = 16.617 \times 10^{-8} \cdot M_{ri} \quad (1)$$

244 Ignition heat flux at each instant (I , kW m⁻²) can be expressed (Eqn 2) assuming that the heat
245 generated by the charcoal combustion is homogeneously transmitted through all the transferring
246 area of the charcoal volume:

247
$$I = \frac{\dot{Q}_t}{A} = \frac{\dot{M}_i \cdot H_c}{A} \quad (2)$$

248 where \dot{Q}_t is the energy released by time (kW) and A is the heat transferring area (0.16 m²
249 corresponding to 5 out of 6 faces of the charcoal volume; there was a 20 × 30-cm section
250 protected by firebreaks acting as insulation).

251 H_c is the heat of combustion of the charcoal (MJ kg⁻¹ of charcoal). Composition of 75% of
252 fixed carbon content (%C) and 20% of volatile matter (%VM) – being the rest 5% ash and
253 moisture content– can be expected for typical charcoal (Food and Agriculture Organization of
254 the United Nations 1984), hence H_c can be obtained by considering the contribution of both heat
255 of char smouldering combustion and heat content of volatile matter as follows:

256
$$H_c = 10^{-2} (\%C \cdot H_{ch} + \%VM \cdot H_{vm}) \quad (3)$$

257 where H_{ch} is the heat of char smouldering combustion (MJ kg⁻¹ of C), and H_{vm} is the heat
258 content of volatile matter (MJ kg⁻¹ of VM). H_{ch} depends on the efficiency of C oxidation, and
259 can be estimated by the products of combustion CO/CO₂ ratio (de Souza Costa and Sandberg
260 2004). According to this, H_{ch} will vary between 21.8 and 29.1 MJ kg⁻¹ of C if a wide range
261 (e.g. 1/3–3) of CO/CO₂ proportion is considered (note that typical values of CO/CO₂ ratios in
262 smouldering combustion are around unity (Rein 2009)). In contrast, heat content of volatile
263 matter (H_{vm}) is mostly comprised between 12.8 and 17.2 MJ kg⁻¹ for most forest fuels (Susott
264 *et al.* 1975; Susott 1982). Thus, with the charcoal composition considered and following Eqn 3, a
265 maximum value of H_c of 25.3 MJ kg⁻¹ of charcoal will be expected if all the C and the VM
266 react and upper bounds of H_{ch} and of H_{vm} are considered. By contrast, taking the lower H_{ch}
267 bound and considering that volatiles might also exit the smouldering surface without reacting

268 (no contribution of H_{vm} in Eqn 3), H_c can have a minimum value of 16.4 MJ kg^{-1} . Therefore,
269 given these H_c limits, a mean value of 20.85 MJ kg^{-1} was assumed for H_c in this study.

270 *Smouldering combustion monitoring*

271 An array of K-type metal-sheathed thermocouples of 0.5-mm diameter, 30-cm length
272 connected to HOB0 Onset U12–014 data loggers was used to monitor soil temperatures. The
273 thermocouples distribution was set (i) according to the sensors availability; (ii) considering two
274 different depths (5 and 15 cm) *a priori* set by analysing preliminary soil moisture content
275 measurements; (iii) depicting a homogenous layout (see Fig. 3). The final array was designed to
276 detect ignition (by observing the temperature evolution of the thermocouple placed 5 cm apart
277 from the ignition source) and to identify any possible heat front spreading laterally and/or
278 downwards (by observing the temperature evolution provided by the rest of the sensors). The
279 loggers were set before the start of the experiments, to acquire temperatures at a frequency of
280 one datum per minute.

281 In addition to the thermocouples, the experiments were monitored with an IR camera
282 (AGEMA Thermovision 570-Pro, FSI-FLIR Systems) operating at the 7.5–13- μm range. We
283 surveyed the plots at regular time intervals saving nadir viewing images approximately every
284 24 h. The monitoring frequency was determined according to the smouldering activity observed
285 (i.e. low intensity) and according to the overall logistics of the experiments (the study site was
286 located in a remote area). Burning candles were placed at the plot corners and used as hot
287 control points for IR imagery sizing. IR images were analysed using ThermoCAM Researcher
288 software and AutoCAD software. Both the charcoal and the plot surface were modelled as black
289 bodies (Prat-Guitart *et al.* 2015), with emissivity equal to 0.97

290 *Environmental variables*

291 Weather conditions (air temperature, relative humidity 2-m wind speed and direction) were
292 continuously recorded at a frequency of 30 s with a portable weather station (Kestrel 4500) that
293 was placed between the two blocks of plots.

294 Soil moisture content (on dry base) was measured with a Hydrosense Soil Water
295 Measurement System (Campbell Scientific, Inc.) at 12- and 20-cm soil depth. At each block,
296 two points were measured every day just before ignition, one in the corresponding control plot
297 of that burning day and another one outside the block. Two soil samples of $10 \times 10 \times 25 \text{ cm}$
298 (one from each block) were used to calibrate the Hydrosense for the local soil conditions
299 (Supplementary information). The calibration was performed by using a natural dry-down
300 method, measuring the moisture and weighting the soil every 4 h for 4 days. After the 4 days,

301 soil was oven-dried at 80°C until constant weight. Significant differences between days, blocks
302 and soil depth moistures were evaluated using a multifactorial ANOVA.

303 Five soil cores of known volume (62.5 cm³) were extracted with a core sampler of 50-mm
304 diameter and 10-cm depth sampled at each experimental block for calculating bulk density, soil
305 carbon content and mineral content. Samples were taken to the laboratory and oven-dried at
306 80°C until constant weight. The samples were crushed and sieved to 2 mm to remove stones,
307 and the remaining fine roots were removed manually. Bulk density was calculated as the free-
308 stone and free-roots mass fraction per cubic centimetre. A sub-sample was ground and
309 analysed for organic carbon with a mass spectrometer coupled to an elemental analyser (Isotope
310 Ratio Mass Spectrometry) **Finnigan Delta plus XP** at the University of Saint Andrews (UK).
311 Soil inorganic content was determined by weighting the remaining material after burning a 10-g
312 soil subsample on a muffle furnace (**1807 FLIBL CM**) at 1300°C. Soil properties between sites
313 (bulk density, organic carbon and mineral content) were tested for significant differences using
314 a *t*-test for independent samples.

315 Statistical analyses were used using R software (R Foundation for Statistical Computing,
316 Vienna, Austria, see <https://www.R-project.org>).

317 *Experimental results*

318 *(i) Weather variables and soil properties*

319 Weather variables showed the same daily pattern during all burning days. During daytime
320 (i.e. between 7 and 17 h), ambient conditions showed rapid fluctuations in temperature, wind
321 speed and relative humidity (**Fig. 4**). At night time, weather was more stable, with temperature
322 ~8°C, relative humidity above 85% and wind speed between 5 and 9 km h⁻¹ for the whole
323 experimental period (**Fig. 4**).

324 At the study sites, soil had 66% of sand, 22% of silt, and 12% of clay. Soil properties at the
325 sites presented some degree of heterogeneity (**Table 2**), but there were not significant
326 differences between sites in either soil bulk density (*t*-test parameters: $t = 3.18$, d.f. = 8, $P =$
327 0.86), organic carbon (*t*-test parameters: $t = 2.17$, d.f. = 7, $P = 0.39$) and inorganic content (*t*-test
328 parameters: $t = 2.23$, d.f. = 8, $P = 0.55$). These three variables had 34%, 39% and 16%
329 coefficient of variation respectively. Soil moisture content was also relatively constant at the
330 experimental site with no significant differences between days (*F*-test parameters: $F = 1.575$,
331 d.f. = 3, $P = 2.52$) or blocks (*F*-test parameters: $F = 1.28$, d.f. = 1, $P = 2.81$), but soil moisture at
332 20 cm was significantly lower than soil moisture at 12-cm depth (*F*-test parameters: $F = 10.9$,
333 d.f. = 1, $P = 0.003$).

334 (ii) Ignition source and smouldering monitoring

335 At the beginning of the test, the initial charcoal ignition power was $\sim 22 \text{ kW m}^{-2}$, and mean
336 temperature $\sim 434^\circ\text{C}$ (Fig. 5), which translated to a radiative heat flux of 14 kW m^{-2} (following
337 Stefan–Boltzmann Law), that is 60% of the total power initially supplied. According to Eqns 1
338 and 2 and to empirical evidence, charcoal was totally consumed (98%) through smouldering
339 combustion 6.5 h after ignition. During the first 120 min (in which 70% of the charcoal was
340 consumed), average ignition power reached 13 kW m^{-2} , and then decreased to 7 kW m^{-2} with an
341 exponential decay of the burning rate from 10 to 3 g min^{-1} . The remaining fuel was then slowly
342 consumed at a mean burning rate of 1 g min^{-1} supplying 2.28 kW m^{-2} of mean heat flux.

343 Twelve out of the eighteen tests registered temperatures above 60°C at the first thermocouple
344 located 15-cm depth (i.e. TC1 at 3) (Table 3). The time needed for TC1 thermocouples to reach
345 this temperature varied from 8 to 16 h after ignition, depending on the plot. Slightly less than
346 half of these TC1 thermocouples reached 80°C , and three of them registered temperatures above
347 100°C . One TC1 thermocouple registered peak temperatures above 400°C . Three of the
348 thermocouples located at 10 cm from the ignition source (named TC2 or TC3 in Fig. 3)
349 recorded temperatures above 60°C and only in one of these peak temperature reached 80°C .

350 These results show that under our experimental conditions, there was a 6% chance for a weak
351 ground fire ignition (i.e. a ground fire that may propagate less than 10 cm from the ignition
352 point tending to self-extinguish). Furthermore, there was 17% chance of developing a heat front
353 with an average temperature of 60°C that would travel less than 15 cm.

354 From all tests, test B1 in block W1 (i.e. W1B1) registered the highest temperature for the
355 longest sustained period of time (Fig. 6). In that test, soil surrounding TC1 experienced
356 temperatures above 400°C for more than 5 h, reaching a maximum temperature of 463°C at 15 h
357 after ignition, and sustained temperatures exceeding 200°C for 16 h. Other selected TC1
358 thermocouples also registered high temperatures over long periods of time (Fig. 6). For
359 example, test W2D4 registered temperatures above 60°C for more than 45 h, and exhibited a
360 plateau at $80\text{--}100^\circ\text{C}$ (corresponding to soil moisture evaporation) for ~ 12 h. Test W2A3 TC1
361 registered temperatures above 60°C for ~ 15 h. Finally, test W1D1 provides a clear example of
362 an unsuccessful ignition, i.e. although TC1 surpassed the lower dehydration threshold, it
363 registered a clear temperature drop 11 h after ignition.

364 We obtained an indicator of the heat accumulated over time in the soil (referred here as
365 ‘thermal dose’, and elsewhere as ‘integrated area over a 60°C threshold’ (Kennard *et al.* 2005;
366 Bova and Dickinson 2008) for the 15 thermocouples that registered temperatures above 60°C ,
367 by integrating their temperature function within the time range for which temperature was above

368 60°C (Fig. 6c). There was a good linear relationship ($R^2 = 0.978$) between thermal dose and
369 time above 60°C on those plots where the minimum temperature for triggering the smouldering
370 process was not reached, whereas the points of plots that reached smouldering fell outside the
371 linear regression line.

372 Infrared imagery allowed us to control the course of the experiments and to gather
373 information about other smouldering activity not detected by the thermocouples, revealing
374 smouldering combustion in the soil subsurface layers. For instance, in the left lower corner of
375 W1B1 (a section not monitored by thermocouples) a 6.8 cm-long 21.7 cm wide area (49 cm²)
376 with aboveground minimum temperatures of 60°C (maximum value of 78°C) was observed,
377 providing evidence of the existence of a smouldering front located at a certain depth within the
378 plot (Fig. 7). After visual inspection of the soil, we located the affected zone 2.5 cm below the
379 surface and we estimated a mean burnt depth of 2 cm. With this figures we estimated that the
380 solid volume burnt by smouldering was of 98 cm³.

381 Discussion

382 This study presents, for the first time, a systematic methodology for smouldering combustion
383 field experimentation, by which data on the different phases that characterise smouldering fires
384 on organic soils can be gathered. With our method, we were able to identify the transition to the
385 oxidation phase and observed continuous smouldering combustion during ~9 h at 15-cm depth,
386 in a 260-kg m⁻³ dense soil with mean moisture values of 114.5% in Andean grasslands soils
387 exposed to real weather conditions.

388 *Ignition source suitability*

389 The heat flux supplied for ignition in smouldering tests is a key aspect when designing a
390 smouldering experimental method. The ignition limit depends both on the amount of energy
391 transferred from the ignition source to the fuel and on the duration of this heat transfer process.
392 Increasing the power of the ignition source (both in terms of energy or exposure time) may
393 allow starting smouldering at increasing moisture contents (Hawkes 1993; Huang *et al.* 2015).
394 This is particularly important on small-scale laboratory experiments, where the smouldering
395 front spread is physically limited and therefore there must be an ignition method powerful
396 enough for generating sustained smouldering combustion but not too powerful as to interfere
397 with the natural heat transfer process in the sample. To date, this issue has received little
398 attention among the scientific literature, with none or very limited information about ignition
399 power supplied in many studies (Frandsen 1987, 1991; 1997; Reardon *et al.* 2007; Miyanishi
400 and Johnson 2002). The ignition heat flux can be estimated in other studies, (Garlough and
401 Keyes 2011; Rein *et al.* 2008; Prat *et al.* 2015) but to the authors' knowledge, only a few studies

402 report directly on this key parameter (Hawkes 1993; Benschoter *et al.* 2011; Hadden *et al.* 2013;
403 Huang *et al.* 2015).

404 The ignition method presented by here represents a natural ignition scenario, as many ground
405 fires start with an element burning in a soil fissure (e.g. stumps, burning piles of slash, thick
406 trunks, etc.). Ignition power supply has been estimated considering typical values of charcoal
407 composition, CO/CO_2 ratio and heat of oxidation of char and volatiles. The method used to
408 calculate ignition power supply is simple and hence has some uncertainty, mainly related to the
409 hypothesis of assuming that the heat generated by the charcoal combustion is homogeneously
410 transmitted through all the transferring area of the charcoal volume. Our ignition protocol
411 allows to easily estimate total and radiative heat flux, and can be applicable to other soil
412 conditions (e.g. different soil types, bulk density, fuel moisture content). Ohlemiller (2002)
413 established a power limit of $10 \text{ kW} \cdot \text{m}^{-2}$ for achieving sustained smouldering combustion in
414 solid wood, and our method had higher heat fluxes than this threshold for the first 2 h of
415 combustion. At laboratory scale, the most commonly used ignition source is an electrically
416 heated element running along one side of the sample and buried in it to some extent (Frandsen
417 1987, 1991; 1997; Reardon *et al.* 2007; Rein *et al.* 2008; Garlough and Keyes 2011). With the
418 information provided in these studies, we estimate that typical ignition heat flux values in
419 laboratory-based studies range between 1.7 to 20 kW m^{-2} with time exposures ranging from 2 to
420 50 min. Our ignition method therefore provides a longer more accumulated heat flux than
421 laboratory tests.

422 Field experimentation allows working with larger plots than in laboratory, hence minimising
423 possible interferences by the ignition source to the heat transfer process in the smouldering
424 front. Here, we used 0.25-m^2 experimental plots, while sample dimension values on laboratory
425 experiments range between $2.5 \times 10^{-3} \text{ m}^2$ and 0.04 m^2 . Furthermore, field scale avoids extra
426 concerns regarding the border effect, which conversely has to be considered at laboratory scale,
427 by using non-combustible insulating materials of similar thermal properties to the ones of the
428 fuel tested.

429 *Smouldering monitoring by thermocouples and IR imagery*

430 Our combined smouldering monitoring system (i.e. temperature measurements by
431 thermocouples and ground surface thermal imagery), provided to be satisfactory because both
432 systems delivered complementary information needed for a comprehensive study on
433 smouldering combustion.

434 The use of punctual temperature measurements allowed us to observe the different
435 smouldering stages in selected locations of the soil. For example, looking at data from

436 thermocouple TC1 (located 5 cm apart from the ignition source and 15-cm soil depth), we got
437 information about the first phase of the smouldering combustion. Looking at TC1-W1B1, we
438 observed that the dehydration front arrived rapidly at this point (less than 1 h after ignition) and
439 dried the soil for ~2.5 h, which corresponds to the time span of the plateau observed ~80°C.
440 This pre-heating process lasted longer in TC1-W2D4, where a plateau at ~70°C was not
441 observed until 12 h after ignition and the soil did not experience a pronounced temperature
442 increase until 20 h after the beginning of the test. Because the time spans of the temperature
443 plateaus around dehydration temperatures are proportional to moisture content (Rein *et al.*
444 2008), these plateaus in our study likely reflect evidence of differences on moisture content
445 between plots. However, in our experiment the soil moisture of every burned plot was not
446 measured to avoid disturbance of the soil properties. Therefore, further research is needed to
447 corroborate this prediction.

448 Pyrolysis and ignition temperatures of the combustion products (i.e. volatiles and char)
449 depend on the chemical composition and state of the biomass and on the soil heating rate
450 (Miyaniishi 2001; Usup *et al.* 2004; Chen *et al.* 2011). Pyrolysis has been reported to start above
451 150°C in mountain forest peat (Chen *et al.* 2011). According to this threshold (looking at TC1
452 behaviour, Fig. 6a) pyrolysis in W1B1 started 4.5 h after the beginning of the test at the TC1
453 spot, whereas it would not have been triggered in W2D4 (maximum temperature registered by
454 TC1-W2D4 was 138°C 24.7 h after the beginning of the test). Ignition reflects the transition
455 between endothermic to exothermic processes (Frandsen 1997) and, as such, ignition
456 temperature can be thought of as the point between both (Usup *et al.* 2004). Usup *et al.* (2004)
457 found ignition temperatures of volatiles in smouldering experiments of tropical peatlands
458 between 250 and 280°C and ignition temperatures of char between 340 and 370°C. In W1B1
459 ignition occurred ~10 h after the beginning of the test when TC1 registered the local minimum
460 of 285°C and temperature increased abruptly immediately afterwards, as a result of the
461 exothermic oxidation of the pyrolysis products (Fig. 6c). If we consider this instant as the
462 smouldering front characteristic arrival time, we can estimate that the smouldering front covered
463 5 cm at ~5 mm h⁻¹. This value corresponds to a self-extinguishing ground fire front and is below
464 the typical ranges for smouldering fronts of 10–30 mm h⁻¹ (Rein 2009).

465 In smouldering peat fires, heat is transferred to the surface soil layer over periods of time of
466 the order of 1 h, which can lead to soil sterilisation (Grishin *et al.* 2009). With our
467 thermocouples readings, we have observed residence times of temperatures above 80–100°C of
468 ~22 h, in both ignited and non-ignited plots, at 15-cm depth. In compacted soils and deep layers
469 heat losses are minimised, and as such residence times are significantly higher. Those values,
470 however, have never been reported before in laboratory studies. Such high temperatures can

471 have important ecological effects on the soil, such a microbial biota death, protein degradation
472 and soil disaggregation (Cerdà and Robichaud 2009).

473 The large series of experiments with multiple replications at the Puna soil revealed weak
474 ignition conditions (only the first few thermocouples registered heat transfer processes signals),
475 which probably indicates that ground fires have very low incidence and mild consequences in
476 Andean Puna under conditions similar to that of the experiments. Nevertheless, having densely
477 monitored experiments (i.e. 7 thermocouples in a 375-cm² area at two different depths) would
478 have allowed us to eventually detect the lateral as well as the downward propagation edge in a
479 volume of 5600 cm³ of soil in each plot. The optimum thermocouples layout depends on the
480 organic horizon depth and on the soil properties governing ignition and spread of the
481 smouldering front. Most of this information is *a priori* unknown, so there is not a definitive
482 sensor arrangement that will suit all types of soils. However, distances of 5–10 cm between
483 thermocouples at representative depths might be adequate to have a clear representation of the
484 smouldering edge spread in most type of soils.

485 The use of IR imagery allowed controlling the experimentation. Monitoring frequency (every
486 24 h) was enough to observe the course of the experiments (a higher frequency would be
487 recommended in case more intense activity was observed). Moreover, it allowed detecting the
488 existence of smouldering subsurface activity in areas not covered by the thermocouples and thus
489 complemented the information given by these. Thermocouples provide point-specific
490 temperature–time evolution and, because of their nature, they cannot cover (and it is not
491 practically feasible) the overall experimental volume. In contrast, IR imagery is surface specific
492 and can be used to assess the overall smouldering activity up to a certain depth. The analysis of
493 IR images coupled with simple visual inspections provided us estimation in an easy and precise
494 way of areas and volumes affected by smouldering in experimental plots, which in turn, permits
495 assessing key parameters related to fuel consumption. Surface radiative temperatures just above
496 60°C depicted in thermal images revealed the presence and the morphology of a smouldering
497 solid volume of 98 cm³ in one of our plots, which would have remained undetected otherwise.
498 Therefore, considering a mean soil organic carbon content of 22.6% in our plots, we can
499 estimate a maximum amount of carbon released in the mentioned solid volume of 5.8 g. This is
500 a conservative figure as combustion efficiency has not been taken into account in this simple
501 calculation.

502 Note that thermal IR imagery can eventually also be used to obtain more detailed
503 smouldering dynamics provided a set of images recorded at an adequate frequency is available.
504 Our experiments did not allow performing such analysis as they were surveyed once every 24 h.

505 Nonetheless, with self-sustained smouldering activity captured in IR images, propagation
506 vectors can be calculated at a fine scale (Prat-Guitart *et al.* 2015, 2016).

507 **Conclusions**

508 This study provides an experimental methodology that represents an important advance for
509 obtaining ground fire behaviour and effects metrics under realistic scenarios. The method
510 provides a detailed picture in terms of smouldering fire combustion dynamics and related
511 parameters under field conditions and can be a good complement to laboratory studies aimed at
512 analysing the particular involvement of a certain soil property on the smouldering ignition and
513 propagation phenomena.

514 The method is to be applied in undisturbed soil under field conditions. The applicability of
515 such a method should comprise many types of subsurface organic layers (i.e. duff, organic rich
516 soils, peatlands), regardless their locations (tropical, temperate or boreal) and is particularly
517 indicated for soils with high densities (difficult to reproduce at laboratory scale), for soils
518 difficult to sample without disturbances, and particularly for soils in remote areas.

519 The experimental protocol is based on a realistic non-electric ignition source whose power
520 supply can be easily estimated. The monitoring system relies on combining both punctual and
521 superficial temperature measurements by which data on smouldering combustion phases and
522 fire behaviour basic descriptors (such as rate of spread or carbon consumed) can be obtained.

523 The methodology presented applied to Andean Puna soils represent a novel contribution,
524 since studies of organic soil consumption by smouldering in the tropical eco-zone are limited.
525 The soil was tested (mean density of 260 kg m⁻³ and mean moisture of 114.5%) by means of
526 large series of replicate experiments which exhibited weak ignition conditions, hence indicating
527 that smouldering fires may have little effect in these type of ecosystems. However, we could
528 observe transition to oxidation phase with smouldering combustion during ~9 h at 15-cm depth
529 and residence times at temperatures above dehydration of ~22 h. This behaviour has never been
530 reported in peer-reviewed laboratory studies.

531 Further work is required to follow-up methodology robustness. Efforts in this regard should
532 be 2-fold; in one hand, method's sensitivity on the ignition source main variables (i.e. charcoal
533 type and mass) should be assessed, and on the other, different soil conditions (i.e. density,
534 moisture and inorganic content) should be also tested using our experimental protocol to
535 confirm its global applicability.

536 **Conflicts of interest**

537 The authors declare that they have no conflicts of interest.

538 **Acknowledgements**

539 This study was funded by the Spanish Ministerio de Economía y Competitividad (projects AGL2011–
540 23425 and CTM2014–57448-R also supported by FEDER funds) and UK Natural Environment Research
541 Council (NE/G006385/1). La Asociación para la Conservación de la Cuenca Amazónica (ACCA) assisted
542 with logistical support and the Autonomous Government of Catalonia (2014-SGR-413) with institutional
543 support. Christian Mata assisted with artwork. The authors thank the comments of Benjamin Blonder and
544 three anonymous reviewers who helped improving the manuscript.

545 **References**

- 546 <bok>Babrauskas V (2003) 'Ignition Handbook.' (Fire Science Publishers: Issaquah, WA, USA)</bok>
- 547 <jrn>Benscoter BW, Vitt DH, Wieder RK (2005) Association of post-fire peat accumulation and
548 microtopography in boreal bogs. *Canadian Journal of Forest Research* **35**, 2188–2193.
549 [doi:10.1139/x05-115](https://doi.org/10.1139/x05-115)</jrn>
- 550 <jrn>Benscoter BW, Thompson DK, Waddington JM, Flannigan MD, Wotton BM, de Groot WJ,
551 Turetsky MR (2011) Interactive effects of vegetation, soil moisture and bulk density on depth of
552 burning of thick organic soils. *International Journal of Wildland Fire* **20**, 418–429.
553 [doi:10.1071/WF0818](https://doi.org/10.1071/WF0818)</jrn>
- 554 <jrn>Bertschi I, Yokelson RJ, Ward DE, Babbitt RE, Susott RA, Goode JG, Hao WM (2003) Trace gas
555 particle emissions from fires in large diameter and belowground biomass fuels. *Journal of Geophysical*
556 *Research* **108**(D13), 8472. [doi:10.1029/2002JD002100](https://doi.org/10.1029/2002JD002100)</jrn>
- 557 <jrn>Bova AS, Dickinson MB (2008) Beyond 'fire temperatures': calibrating thermocouple probes and
558 modelling their response to surface fires in hardwood fuels. *Canadian Journal of Forest Research* **38**,
559 1008–1020. [doi:10.1139/X07-204](https://doi.org/10.1139/X07-204)</jrn>
- 560 <jrn>Bridge SRJ, Johnson EA (2000) Geomorphic principles of terrain organization and vegetation
561 gradients. *Journal of Vegetation Science* **11**, 57–70. [doi:10.2307/3236776](https://doi.org/10.2307/3236776)</jrn>
- 562 <other>Carrington D (2015) Indonesian forest fires on track to emit more CO₂ than UK. *The Guardian*, 7
563 October 2015. Available at <http://www.xxxx> [Verified on 2 November 2017]</other>
- 564 <bok>Cerdà A, Robichaud PR (2009) 'Fire Effects on Soils and Restoration Strategies.' (CRC Press,
565 Taylor & Francis Group: Boca Raton, FL, USA)</bok>
- 566 <jrn>Chen H, Zhao W, Liu N (2011) Thermal analysis and decomposition kinetics of Chinese forest peat
567 under nitrogen and air atmospheres. *Energy & Fuels* **25**, 797–803. [doi:10.1021/ef101155n](https://doi.org/10.1021/ef101155n)</jrn>
- 568 <jrn>Conard SG, Sukhinin AI, Stocks BJ, Cahoon DR, Davidenko EP, Ivanova GA (2002) Determining
569 effects of area burned and fire severity on carbon cycling and emissions in Siberia. *Climatic Change*
570 **55**, 197–211. [doi:10.1023/A:1020207710193](https://doi.org/10.1023/A:1020207710193)</jrn>

- 571 <jrn>Costa FS, Sandberg D (2004) Mathematical model of a smoldering log. *Combustion and Flame* **139**,
572 227–238. [doi:10.1016/j.combustflame.2004.07.009](https://doi.org/10.1016/j.combustflame.2004.07.009)</jrn>
- 573 <jrn>Davies GM, Gray A, Rein G, Legg CJ (2013) Peat consumption and carbon loss due to smouldering
574 wildfire in a temperate peatland. *Forest Ecology and Management* **308**, 169–177.
575 [doi:10.1016/j.foreco.2013.07.051](https://doi.org/10.1016/j.foreco.2013.07.051)</jrn>
- 576 <jrn>Davies GM, Domènech R, Gray A, Johnson PCD (2016) Vegetation structure and fire weather
577 influence variation in burn severity and fuel consumption during peatland wildfires. *Biogeosciences*
578 **13**, 389–398. [doi:10.5194/bg-13-389-2016](https://doi.org/10.5194/bg-13-389-2016)</jrn>
- 579 <jrn>de Groot WJ, Pritchard JM, Lynham TJ (2009) Forest floor fuel consumption and carbon emissions
580 in Canadian boreal forest fires. *Canadian Journal of Forest Research* **39**(2), 367–382.
581 [doi:10.1139/X08-192](https://doi.org/10.1139/X08-192)</jrn>
- 582 <edb>Food and Agriculture Organization of the United Nations (1987) Using charcoal efficiently. In
583 ‘Simple Technologies of Charcoal Making’. FAO , pp. 101–107. (Food and Agriculture Organization
584 of the United Nations.).</edb>
- 585 <jrn>Filkov AI, Kuzin AY, Sharpov OV, Leroy-Cancellieri V, Cancellieri D, Leoni E, Simeoni A, Rein
586 G (2012) A comparative study to evaluate the drying kinetics of boreal peats from micro to macro
587 scales. *Energy & Fuels* **26**, 349–356. [doi:10.1021/e201221v](https://doi.org/10.1021/e201221v)</jrn>
- 588 <jrn>Frandsen WH (1987) The influence of moisture and mineral soil on the combustion limits of
589 smouldering forest duff. *Canadian Journal of Forest Research* **17**(12), 1540–1544. [doi:10.1139/x87-
590 236](https://doi.org/10.1139/x87-236)</jrn>
- 591 <jrn>Frandsen WH (1991) Heat evolved from smoldering peat. *International Journal of Wildland Fire*
592 **1**(3), 197–204. [doi:10.1071/WF9910197](https://doi.org/10.1071/WF9910197)</jrn>
- 593 <jrn>Frandsen WH (1997) Ignition probability of organic soils. *Canadian Journal of Forest Research*
594 **27**(9), 1471–1477. [doi:10.1139/x97-106](https://doi.org/10.1139/x97-106)</jrn>
- 595 <jrn>Frandsen WH (1998) Heat flow measurements from smoldering porous fuel. *International Journal*
596 *of Wildland Fire* **8**(3), 137–145. [doi:10.1071/WF9980137](https://doi.org/10.1071/WF9980137)</jrn>
- 597 <jrn>Garlough EC, Keyes CR (2011) Influences of moisture content, mineral content and bulk density on
598 smoldering combustion of ponderosa pine duff mounds. *International Journal of Wildland Fire* **20**,
599 589–596. [doi:10.1071/WF10048](https://doi.org/10.1071/WF10048)</jrn>
- 600 <jrn>Gibbon A, Silman M, Malhi Y, Fisher J, Meir P, Zimmermann M, Dargie GC, Farfan WR, Garcia
601 KC (2010) Ecosystem carbon storage across the Grassland–Forest transition in the high Andes of
602 Manu National Park, Peru. *Ecosystems* **13**(7), 1097–1111. [doi:10.1007/s10021-010-9376-8](https://doi.org/10.1007/s10021-010-9376-8)</jrn>
- 603 <jrn>Grishin AM, Yakimov AS, Rein G, Simeoni A (2009) On physical and mathematical modeling of
604 the initiation and propagation of peat fires. *Journal of Engineering Physics and Thermophysics* **82**(6),
605 1235–1243. [doi:10.1007/s10891-010-0293-7](https://doi.org/10.1007/s10891-010-0293-7)</jrn>

- 606 <jrn>Hadden RM, Rein G, Belcher CM (2013) Study of the competing chemical reactions in the
607 initiation and spread fo smouldering combustion in peat. *Proceedings of the Combustion Institute* **34**,
608 2547–2553. doi:10.1016/j.proci.2012.05.060</jrn>
- 609 <ths>Hawkes BC (1993) Factors that influence peat consumption under dependent burning conditions: a
610 laboratory study. PhD dissertation, School of Forestry, University of Montana, Missoula, MT,
611 USA.</ths>
- 612 Huang, X, Rein G (2015) Computational study of critical moisture and depth of burn in peat fires.
613 *International Journal of Wildland Fire* **24**, 798-808. doi: 10.1071/WF14178
- 614 <jrn>Huang X, Rein G, Chen H (2015) Computational smouldering combustion: predicting the roles of
615 moisture and inert contents in peat wildfires. *Proceedings of the Combustion Institute* **35**, 2673–2681.
616 doi:10.1016/j.proci.2014.05.048</jrn>
- 617 <jrn>Huang X, Restuccia F, Gramola M, Rein G (2016) Experimental study of the formation and collapse
618 of an overhang in the lateral spread of smouldering peat fires. *Combustion and Flame* **168**, 393–402.
619 doi:10.1016/j.combustflame.2016.01.017</jrn>
- 620 <jrn>Kennard DK, Outcalt KW, Jones D, O'Brien JO (2005) Comparing techniques for estimating flame
621 temperature of prescribed fires. *Fire Ecology* **1**(1), 75–84. doi:10.4996/fireecology.0101075</jrn>
- 622 <bok>Lawson BD, Frandsen WH, Hawkes BC, Dalrymple GN (1997) Probability of sustained
623 smoldering ignition for some boreal forest duff types. Natural Resources Canada, Canadian Forest
624 Service, Northern Forestry Centre, Forest Management Note 63. (Edmonton, AB, Canada)</bok>
- 625 <edb>Miyanishi K (2001) Duff consumption. In 'Forest Fires: Behaviour and Ecological Effects'. (Eds
626 EA Johnson, K Miyanishi) pp. 437–470. (Academic Press: San Diego, CA, USA)</edb>
- 627 <jrn>Miyanishi K, Johnson EA (2002) Process and patterns of duff consumption in the mixedwood boreal
628 forest. *Canadian Journal of Forest Research* **32**, 1285–1295. doi:10.1139/x02-051</jrn>
- 629 <jrn>Moore S, Evans CD, Page SE, Garnett MH, Jones TG, Freeman C, Hooijer A, Wiltshire AJ, Limin
630 SH, Gauci V (2013) Deep instability of deforested tropical peatlands revealed by fluvial organic
631 carbon fluxes. *Nature* **493**, 660–663. doi:10.1038/nature11818</jrn>
- 632 <jrn>Ohlemiller TJ (1985) Modeling of smoldering combustion propagation. *Progress in Energy and
633 Combustion Science* **11**, 277–310. doi:10.1016/0360-1285(85)90004-8</jrn>
- 634 <edb>Ohlemiller TJ (2002) Smoldering combustion. In 'SFPE Handbook of Fire Protection
635 Engineering', 3rd edn. (Eds P J DiNenno, D Drysdale, C L Beyler and WD Walton) pp. xx–xx.
636 (NFPA).</edb>
- 637 <jrn>Oliveras I, Malhi Y, Salinas N, Huaman V, Urquiaga-Flores E, Kala-Mamani J, Quintano-Loaiza
638 JA, Cuba-Torres I, Lizarraga-Morales N, Román-Cuesta RM (2013) Changes in forest structure and
639 composition after fire in tropical montane cloud forests near the Andean treeline. *Plant Ecology &
640 Diversity* **7**(1–2), 329–340.</jrn>

- 641 <jrn>Oliveras I, van der Eynden M, Malhi Y, Cahuana N, Menor C, Zamora F, Haugaasen T (2014a)
642 Grass allometry and estimation of above-ground biomass in tropical alpine tussock grasslands. *Austral*
643 *Ecology* **39**, 408–415. [doi:10.1111/aec.12098](https://doi.org/10.1111/aec.12098)</jrn>
- 644 <jrn>Oliveras I, Girardin C, Doughty CE, Cahuana N, Arenas CE, Oliver V, Huaraca Huasco W, Malhi
645 Y (2014b) Andean grasslands are as productive as tropical cloud forests. *Environmental Research*
646 *Letters* **9**, 115011. [doi:10.1088/1748-9326/9/11/115011](https://doi.org/10.1088/1748-9326/9/11/115011)</jrn>
- 647 <jrn>Oliveras I, Anderson LO, Malhi Y (2014c) Application of remote sensing to understanding fire
648 regimes and biomass burning emissions of the tropical Andes. *Global Biogeochemical Cycles* **28**(4),
649 480–496. [doi:10.1002/2013GB004664](https://doi.org/10.1002/2013GB004664)</jrn>
- 650 <jrn>Page SE, Siegert F, Rieley JO, Boehm HDV, Jaya A, Limin S (2002) The amount of carbon
651 released from peat and forest fires in Indonesia during 1997. *Nature* **420**, 61–65.
652 [doi:10.1038/nature01131](https://doi.org/10.1038/nature01131)</jrn>
- 653 <edb>Page SE, Hoscilo A, Langner A, Tansey K, Siegert F, Limin S, Rieley J (2009) Tropical peatland
654 fires in Southeast Asia. In ‘Tropical Fire Ecology’. (Ed. MA Cochrane) pp. xx–xx. (Springer:,
655 Chistester, UK)</edb>
- 656 <jrn>Plucinski MP, Pastor E (2013) Criteria and methodology for measuring aerial wildfire suppression.
657 *International Journal of Wildland Fire* **22**, 1144–1154. [doi:10.1071/WF13040](https://doi.org/10.1071/WF13040)</jrn>
- 658 <jrn>Prat N, Belcher C, Hadden R, Rein G, Yearsley J (2015) A laboratory study of the effect of moisture
659 content on the spread of smouldering in peat fires. *Flamma* **6**, 35–38.</jrn>
- 660 <edb>Prat-Guitart N, Belcher CM, Hadden R, Yearsley JM (2015) Infrared analysis as a tool for studying
661 the horizontal smoldering propagation in laboratory peat fires. In ‘Coal and Peat Fires, a Global
662 Perspective, Peat–Geology, Combustion and Case Studies’. (Eds GB Stracher, A Prakash, G Rein) pp.
663 121–139. (Elsevier: Amsterdam, Netherlands)</edb>
- 664 <jrn>Prat-Guitart N, Rein G, Hadden RM, Belcher CM, Yearsley JM (2016) Propagation probability and
665 spread rates of self-sustained smouldering fires under controlled moisture content and bulk density
666 conditions. *International Journal of Wildland Fire* **25**, 456–465.</jrn>
- 667 <jrn>Reardon J, Hungerford R, Ryan K (2007) Factors affecting sustained smouldering in organic soils
668 from pocosin and pond pine woodland wetlands. *International Journal of Wildland Fire* **16**, 107–118.
669 [doi:10.1071/WF06007](https://doi.org/10.1071/WF06007)</jrn>
- 670 <jrn>Reardon J, Curcio G, Bartlett R (2009) Soil moisture dynamics and smoldering combustion limits of
671 pocosin soils in North Carolina, USA. *International Journal of Wildland Fire* **18**, 326–335.
672 [doi:10.1071/WF08085](https://doi.org/10.1071/WF08085)</jrn>
- 673 <jrn>Rein G (2009) Smouldering Combustion Phenomena in Science and Technology. *International*
674 *Review of Chemical Engineering* **1**, 3–18.</jrn>

- 675 <edb>Rein G (2013) Smouldering fires and natural fuels. In 'Fire Phenomena and the earth System: an
676 Interdisciplinary Guide to Fire Science'. (Ed. CM Belcher) pp. 15–34 (Wiley: Oxford, UK)</edb>
- 677 <jrn>Rein G, Cleaver N, Ashton C, Pironi P (2008) The severity of smouldering peat fires and damage to
678 the forest soil. *Catena* **74**(3), 304–309. [doi:10.1016/j.catena.2008.05.008](https://doi.org/10.1016/j.catena.2008.05.008)</jrn>
- 679 <jrn>Román-Cuesta RM, Salinas N, Asbjornsen H, Oliveras I, Huaman V, Gutiérrez Y, Puelles L, Kala J,
680 Yabar D, Rojas M, Astete R, Jordán DY, Silman M, Mosandl R, Weber M, Stimm B, Günter S, Knoke
681 T, Malhi Y (2011) Implications of fires on carbon budgets in Andean cloud montane forest: the
682 importance of peat soils and tree resprouting. *Forest Ecology and Management* **261**, 1987–1997.
683 [doi:10.1016/j.foreco.2011.02.025](https://doi.org/10.1016/j.foreco.2011.02.025)</jrn>
- 684 <jrn>Román-Cuesta RM, Carmona-Moreno C, Lizcano G, New M, Silman M, Knoke T, Malhi Y,
685 Oliveras I, Asbjornsen H, Vuille M (2014) Synchronous fire activity in the tropical high Andes: an
686 indication of regional climate forcing. *Global Change Biology* **20**(6), 1929–1942.
687 [doi:10.1111/gcb.12538](https://doi.org/10.1111/gcb.12538)</jrn>
- 688 <jrn>Susott RA (1982) Characterization of the thermal properties of forest fuels by combustible gas
689 analysis. *Forest Science* **28**(2), 404–420.</jrn>
- 690 <jrn>Susott RA, DeGroot WF, Shafizadeh F (1975) Heat content of natural fuels. *Journal of Fire and*
691 *Flammability* **6**, 311–325.</jrn>
- 692 <jrn>Thompson DK, Wotton BM, Waddington JM (2015) Estimating the heat transfer to an organic soil
693 surface during crown fire. *International Journal of Wildland Fire* **24**, 120–129.
694 [doi:10.1071/WF12121](https://doi.org/10.1071/WF12121)</jrn>
- 695 <jrn>Turetsky MR, Kane ES, Harden JW, Ottmar RD, Maines KL, Hoy E, Kasischke ES (2011) Recent
696 acceleration of biomass burning and carbon losses in Alaskan forests and peatlands. *Nature*
697 *Geoscience* **4**, 27–31. [doi:10.1038/ngeo1027](https://doi.org/10.1038/ngeo1027)</jrn>
- 698 <jrn>Turetsky MR, Benscoter B, Page S, Rein G, Van der Werf GR, Watts A (2014) Global vulnerability
699 of peatlands to fire and carbon loss. *Nature Geoscience* **8**, 11–14. [doi:10.1038/ngeo2325](https://doi.org/10.1038/ngeo2325)</jrn>
- 700 <jrn>Usup A, Hashimoto Y, Takahashi H, Hayasaka H (2004) Combustion and thermal characteristics of
701 peat fire in tropical peatland in Central Kalimantan, Indonesia. *Tropics* **14**(1), 1–19.
702 [doi:10.3759/tropics.14.1](https://doi.org/10.3759/tropics.14.1)</jrn>
- 703 <jrn>Watts AC (2013) Organic soil combustion in cypress swamps: moisture effects and landscape
704 implications for carbon release. *Forest Ecology and Management* **294**, 178–187.
705 [doi:10.1016/j.foreco.2012.07.032](https://doi.org/10.1016/j.foreco.2012.07.032)</jrn>
- 706 <jrn>Yu Z (2012) Northern peatland carbon stocks and dynamics: a review. *Biogeosciences* **9**, 4071–
707 4085. [doi:10.5194/bg-9-4071-2012](https://doi.org/10.5194/bg-9-4071-2012)</jrn>
- 708 <jrn>Zimmermann M, Meir P, Silman M, Fedders A, Gibbon A, Malhi Y, Urrego DH, Bush MB, Feeley
709 KJ, Garcia KC, Dargie GC, Farfan WR, Goetz BP, Johnson WT, Kline KM, Modi AT, Rurau NMQ,

710 **Staudt BT, Zamora F (2010) No differences in soil carbon stocks across the tree line in the Peruvian**
711 **Andes. *Ecosystems* 13(1), 62–74. doi:10.1007/s10021-009-9300-2**</jrn>

712 <other>**Zoltai S, Siltanen R, Johnson J (2000) A wetland database for the western boreal, subarctic, and**
713 **Actic regions of Canada. Canadian Forest Service, Northern Forstry Centre, Report NOR-X-368.**
714 **(Edmonton, AB, Canada)**</other>

715 Manuscript received 13 February 2017, accepted 27 September 2017

716 **Table 1. Tested plots during the three burning days of the experimental campaign**

Tested plots	Day 1 (7-Jul-2012)	Day 2 (11-Jul-2012)	Day 3 (12-Jul-2012)
Plots in block W1	A1, B2, D1	A4, B4, B5	B1, D3, D5
Plots in block W2	B1, C1, C2	B4, D4, C5	A1, A3, A5

717 **Table 2. Range (minimum–maximum) values of the environmental variables associated**
718 **with the ground fire tests**

719 ; DB: dry basis; WB; wet basis.

Variable	Measures
Mean midday ^A temperature (°C)	10.7–18.3
Mean midday windspeed (km h ⁻¹)	6.1–7.9
Mean midday relative humidity (%)	37.7–95.9
Soil moisture content at 12 cm (DB, %)	90.89–130.76
Soil moisture content at 20 cm (DB, %)	83.29–122.96
Mean soil moisture content ^B (DB, %)	114.5
Soil mineral content (%)	6.0–10.6
Soil bulk density (DB, kg m ⁻³)	188–355
Mean soil bulk density (ρ_{WB} , WB, kg m ⁻³)	260
Soil organic carbon (%)	21.1–24.02

720 ^AMidday is considered to be the time interval between 1100 and 1400 hours. ^B Considering measures at
721 all depths

722 **Table 3. Temperature response summary of the tests**

723 TC1 are located at 15-cm depth, 5 cm from the ignition source. TC2 and TC3 are located at 5-
724 cm depth, 10 cm from the ignition source

Thresholds	Number of tests	Occurrence
TC1 at $t > 60^\circ\text{C}$	12/18	67%
TC1 at $t > 80^\circ\text{C}$	5/18	28%
TC1 at $t > 100^\circ\text{C}$	3/18	17%
TC1 at $t > 400^\circ\text{C}$	1/18	6%
TC2/TC3 at $t > 60^\circ\text{C}$	3/18	17%
TC2/TC3 at $t > 80^\circ\text{C}$	1/18	6%

725 **Fig. 1.** Smouldering stages

726 **Fig. 2.** Study area location and sketch of the experimental site. CP1-CP5 are control plots.

727 **Fig. 3.** Scheme of an individual plot showing the ignition procedure. (a) Schematic top view. (b)
728 Schematic side view and (c) picture showing a plot arrangement.

729 **Fig. 4.** Evolution of the weather variables during 24 h of the burning tests (from 1100 hours of 12 July
730 to 1100 hours of 13 July)

731 **Fig. 5.** (a) Ignition source behaviour: fuel consumption, mass loss rate and ignition power; (b)
732 Temperature distribution of burning charcoal at the beginning of test (randomly selected W2_B4).
733 Dashed line delimits the 30 × 10-cm surface area occupied by charcoal. Mean temperature of the
734 delimited area is 434°C (s.d. is 95.3°C)

735 **Fig. 6.** (a) Temperature evolution of TC1 thermocouples at four selected tests; (b) thermal severity
736 registered by the same TC1 thermocouples; (c) thermal dose above 60°C, experienced by TC1, TC2 or
737 TC3 thermocouples in all tests.

738 **Fig. 7.** W1B1 thermal image 24 h after ignition, superimposed on a plot and thermocouples layout.

797 Table 1. Tested plots during the three burning days of the experimental campaign

Tested plots	Day 1	Day 2	Day 3
	(07/07/2012)	(07/11/2012)	(07/12/2012)
Plots in block W1	A1, B2, D1	A4, B4, B5	B1, D3, D5
Plots in block W2	B1, C1, C2	B4, D4, C5	A1, A3, A5

798

799 Table 2. Range (min – max) values of the environmental variables associated with the ground
800 fire tests. ⁽¹⁾ midday is considered to be the time interval between 11.00h and 14.00h; ⁽²⁾

801 Considering measures at all depths; d.b.: dry basis; w.b.; wet basis.

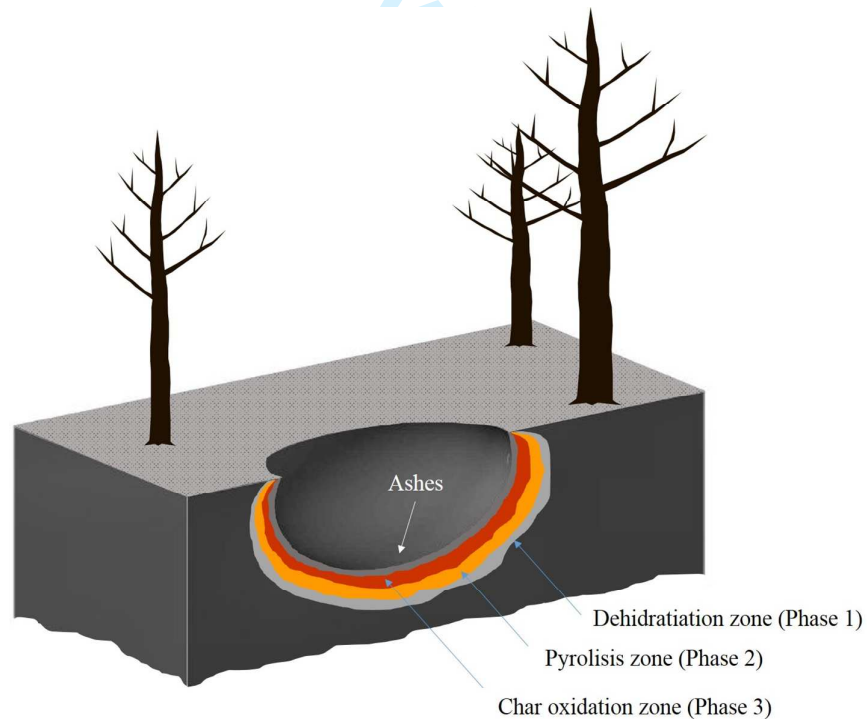
Variable	Measures
Mean midday ⁽¹⁾ temperature (°C)	10.7 – 18.3
Mean midday windspeed (km·h ⁻¹)	6.1 – 7.9
Mean midday relative humidity (%)	37.7 – 95.9
Soil moisture content at 12 cm (d.b.%)	90.89 – 130.76
Soil moisture content at 20 cm (d.b.%)	83.29 – 122.96
Mean soil moisture content ⁽²⁾ (d.b.%)	114.5
Soil mineral content (%)	6.0-10.6
Soil bulk density (d.b. kg·m ⁻³)	188-355
Mean soil bulk density ($\rho_{w.b.}$, w.b. kg·m ⁻³)	260
Soil organic carbon (%)	21.1 – 24.02

802

803 Table 3. Temperature response summary of the tests. TC1 are located at 15 cm depth, 5 cm from
 804 the ignition source. TC2 and TC3 are located at 5 cm depth, 10 cm from the ignition source.

Temperature Thresholds	Number of tests	Occurrence
TC1 at $T > 60^{\circ}\text{C}$	12/18	67%
TC1 at $T > 80^{\circ}\text{C}$	5/18	28%
TC1 at $T > 100^{\circ}\text{C}$	3/18	17%
TC1 at $T > 400^{\circ}\text{C}$	1/18	6%
TC2/TC3 at $T > 60^{\circ}\text{C}$	3/18	17%
TC2/TC3 at $T > 80^{\circ}\text{C}$	1/18	6%

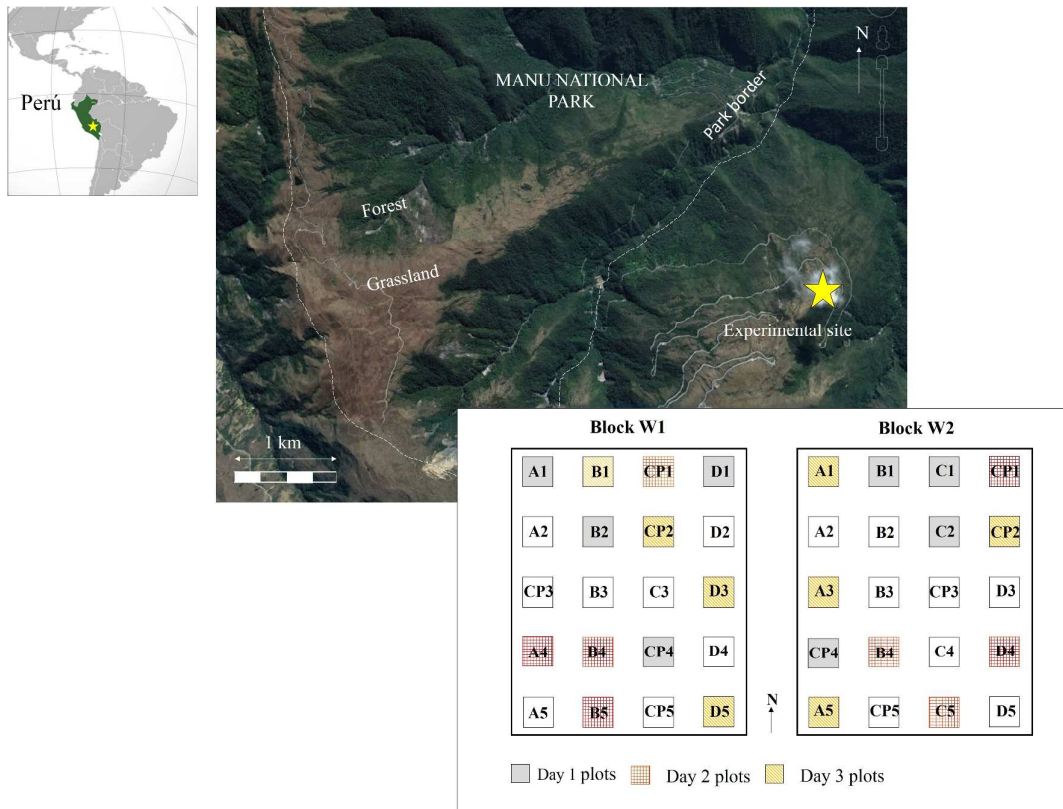
805



806

807 Fig. 1. Smouldering stages

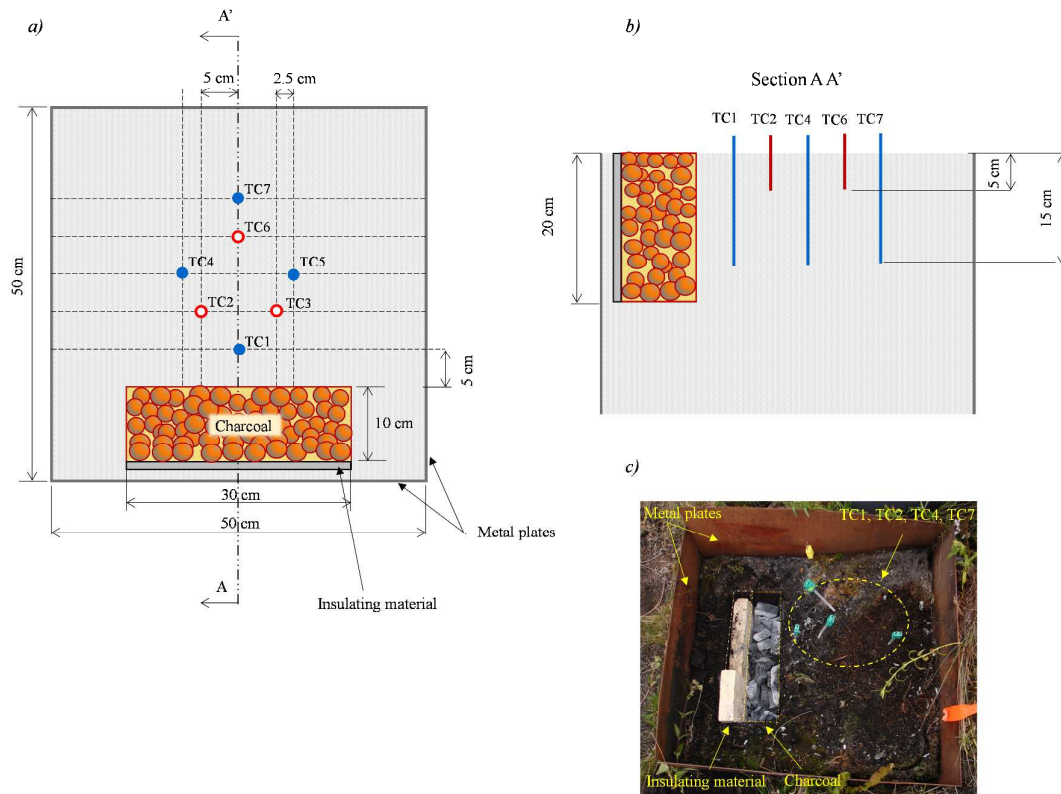
808



809

810 Fig. 2. Study area location and sketch of the experimental site. CP1-CP5 are control plots.

811

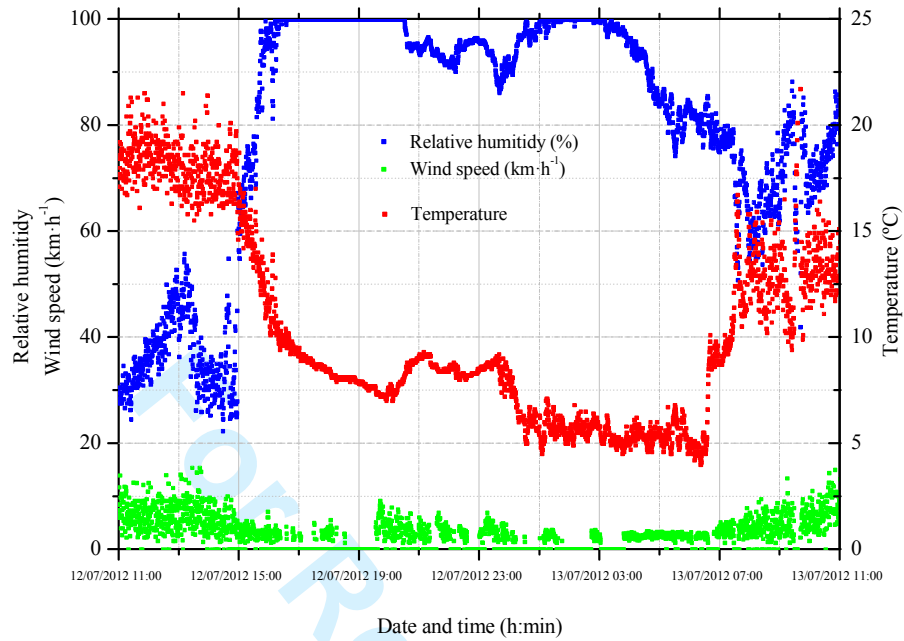


812

813 Fig. 3. Scheme of an individual plot showing the ignition procedure. a) Schematic top view. b)

814 Schematic side view and c) picture showing a plot arrangement.

815

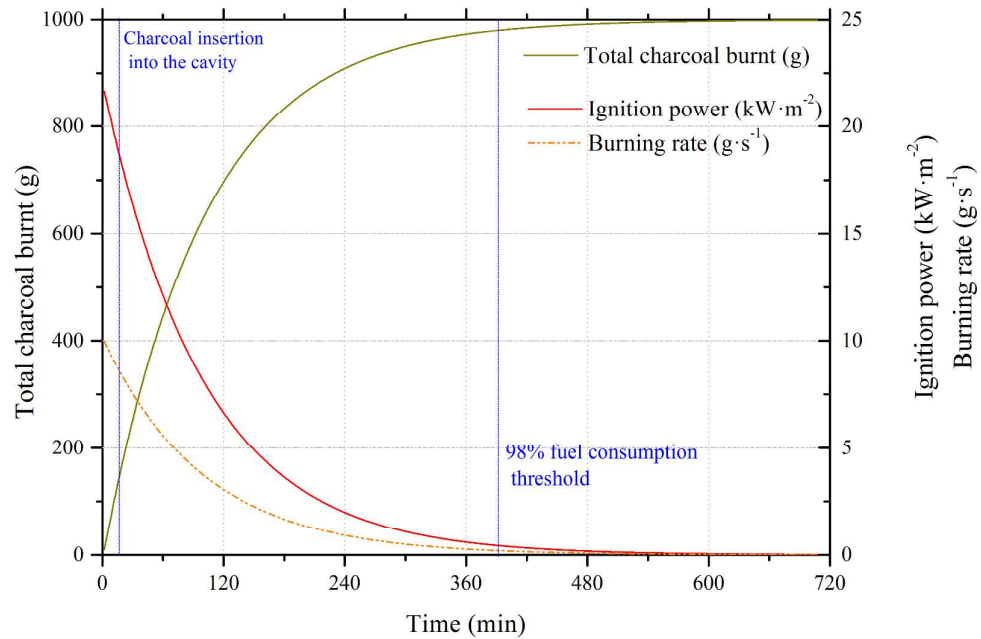


816

817 Fig. 4. Evolution of the weather variables during 24h of the burning tests (from 11.00h of July
818 12th to 11h of July 13th)

819

820 a)



821

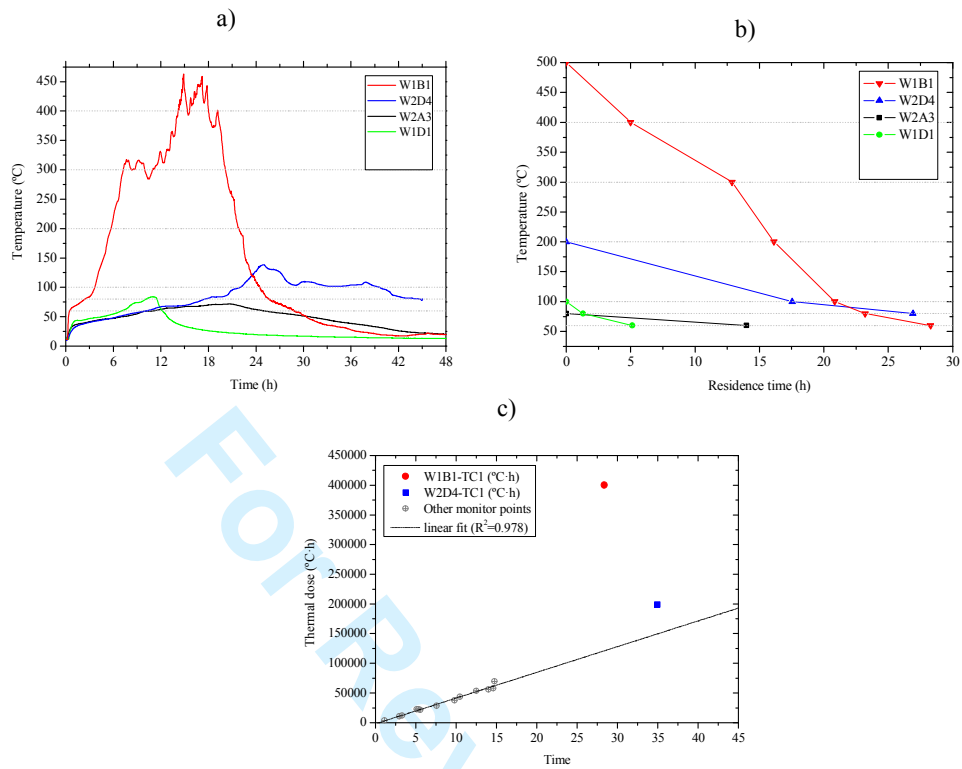
822 b)



823

824 Fig. 5. a) Ignition source behaviour: fuel consumption, mass loss rate and ignition power; b)
 825 Temperature distribution of burning charcoal at the beginning of test (randomly selected
 826 W2_B4). Blue dashed line delimits the 30 cm x 10 cm surface area occupied by charcoal. Mean
 827 temperature of the delimited area is 434°C (st.dv is 95.3°C)

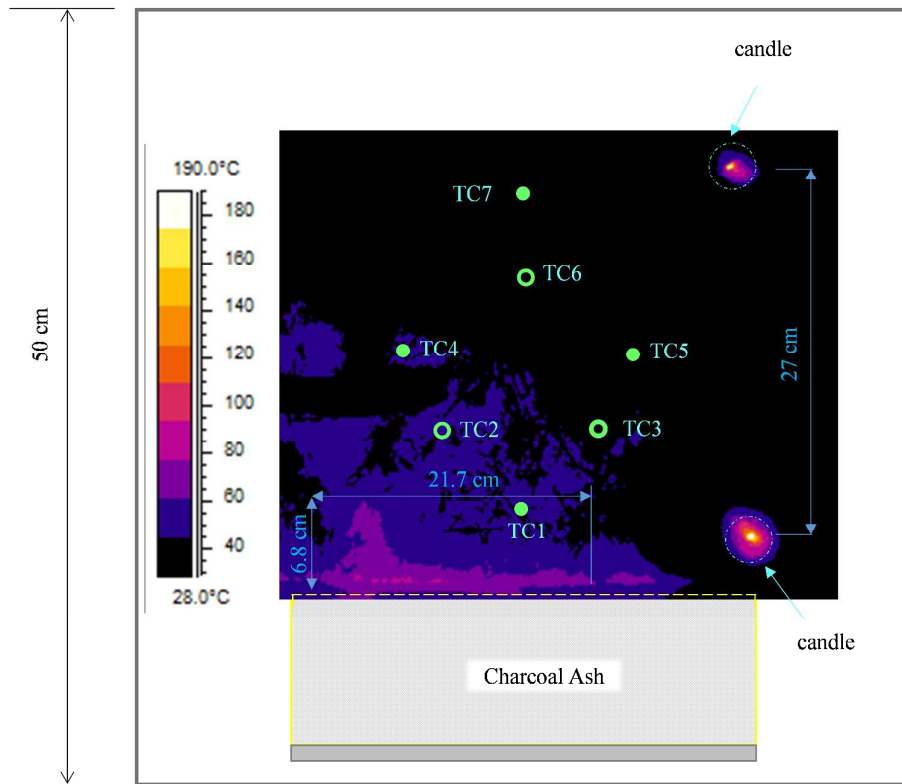
828



829

830 Fig. 6. a) Temperature evolution of TC1 thermocouples at four selected tests; b) thermal
 831 severity registered by the same TC1 thermocouples; c) Thermal dose above 60°C, experienced
 832 by TC1, TC2 or TC3 thermocouples in all tests.

833



834

835 Fig. 7. W1B1 thermal image 24h after ignition, superimposed on a plot and thermocouples

836 layout.

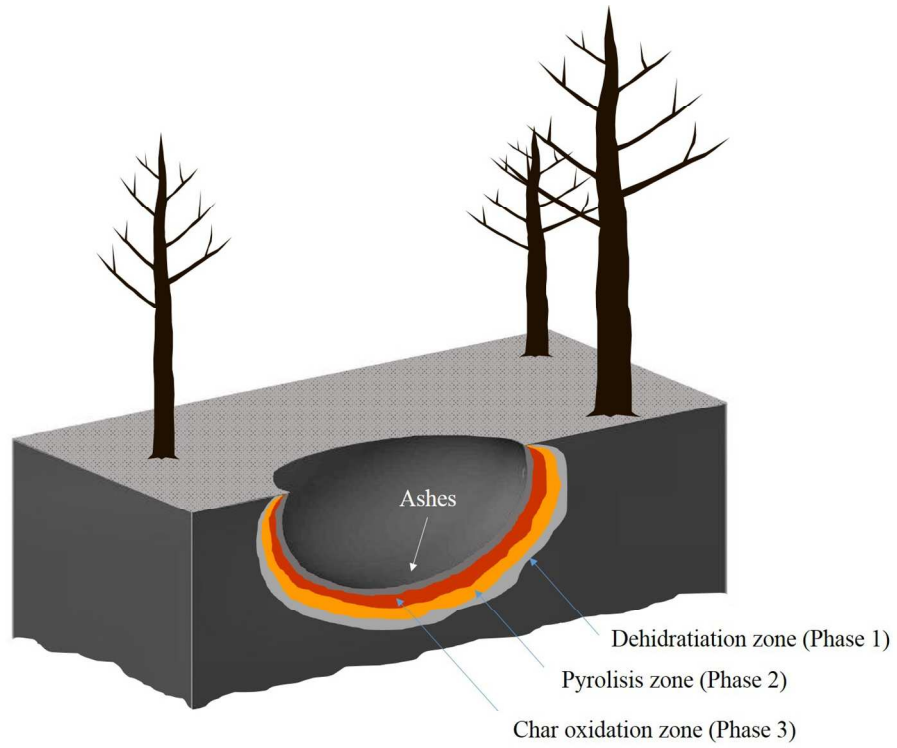
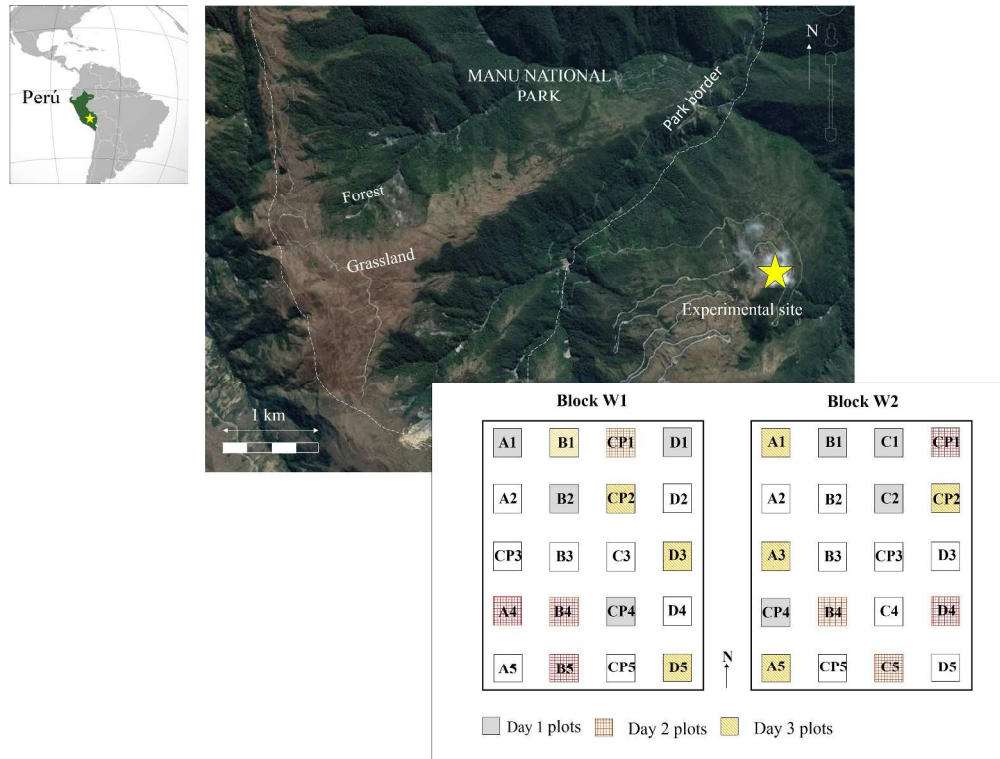


Fig.1. Smouldering stages

272x218mm (150 x 150 DPI)

Only



Study area location and sketch of the experimental site. CP1-CP5 are control plots.

740x558mm (150 x 150 DPI)

Only

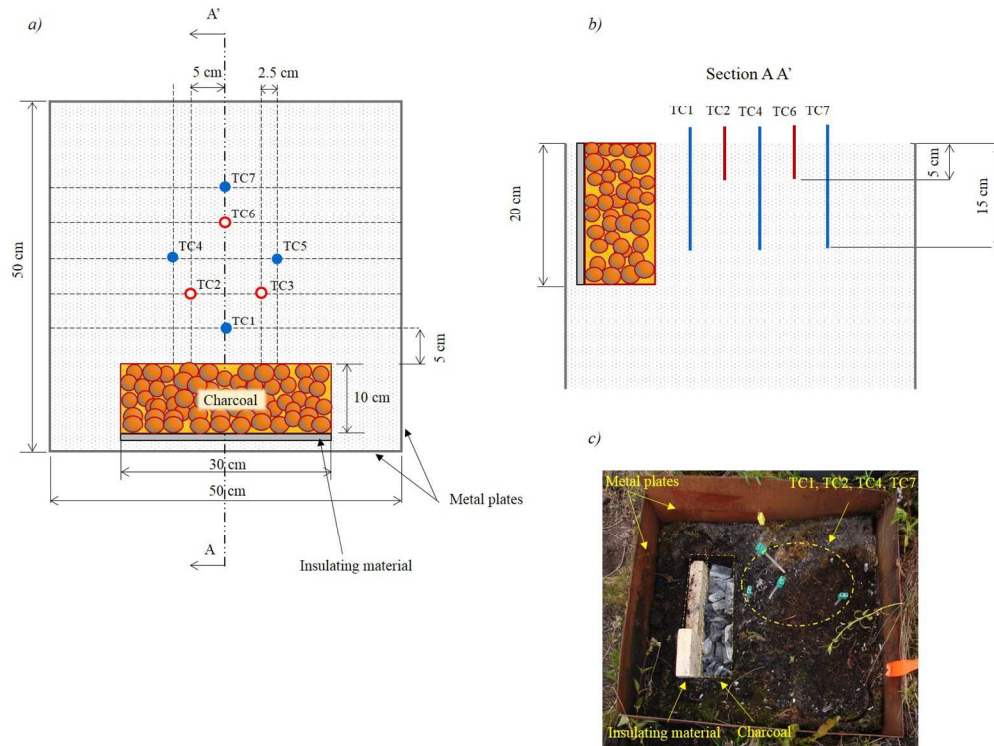


Fig. 3. Scheme of an individual plot showing the ignition procedure. a) Schematic top view. b) Schematic side view and c) picture showing a plot arrangement.

285x213mm (150 x 150 DPI)

Only

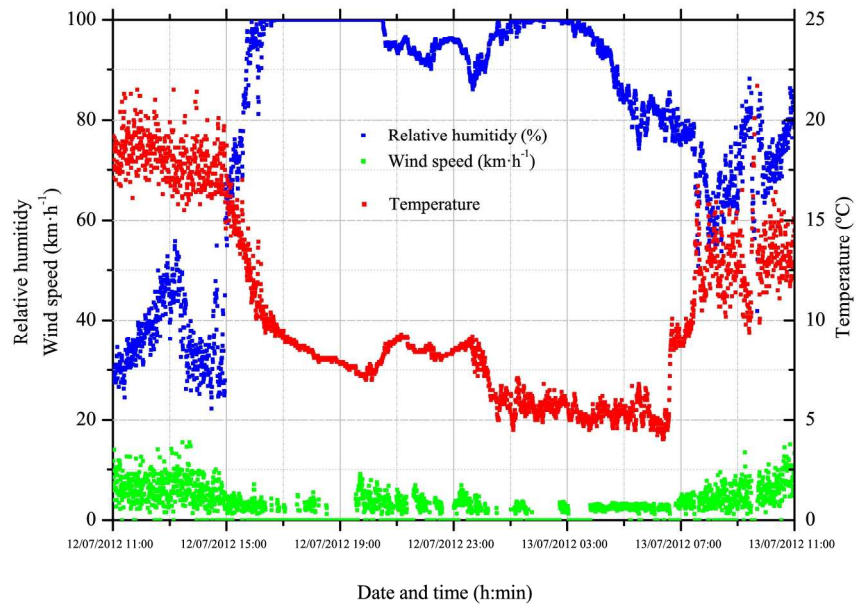
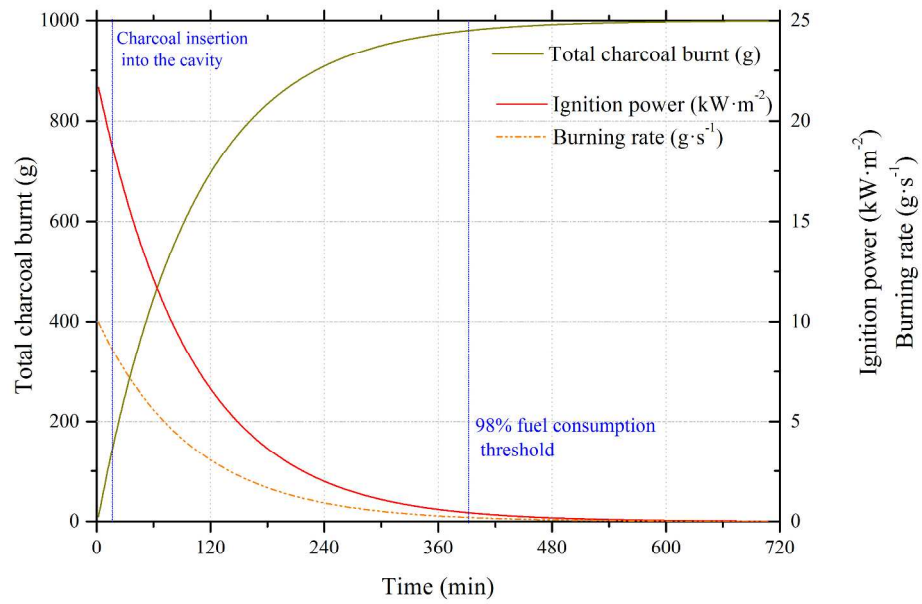


Fig. 4. Evolution of the weather variables during 24h of the burning tests (from 11.00h of July 12th to 11h of July 13th)

201x141mm (300 x 300 DPI)



a) Ignition source behaviour: fuel consumption, mass loss rate and ignition power

288x201mm (300 x 300 DPI)



Fig. 5. b) Temperature distribution of burning charcoal at the beginning of test (randomly selected W2_B4). Blue dashed line delimits the 30 cm x 10 cm surface area occupied by charcoal. Mean temperature of the delimited area is 434°C (st.dv is 95.3°C)

107x63mm (150 x 150 DPI)

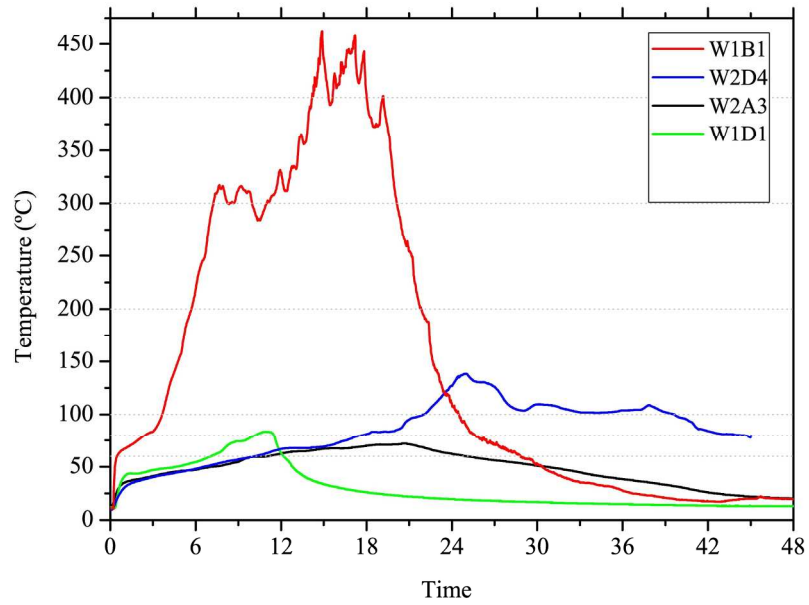


Fig. 6. a) Temperature evolution of TC1 thermocouples at four selected tests.

202x141mm (300 x 300 DPI)

www Only

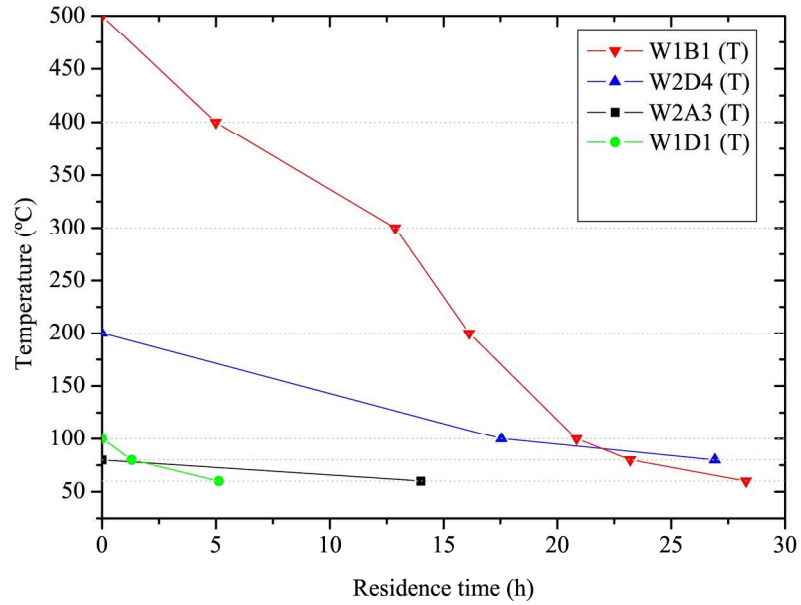


Fig. 6. b) thermal severity registered by the same TC1 thermocouples.

202x141mm (300 x 300 DPI)

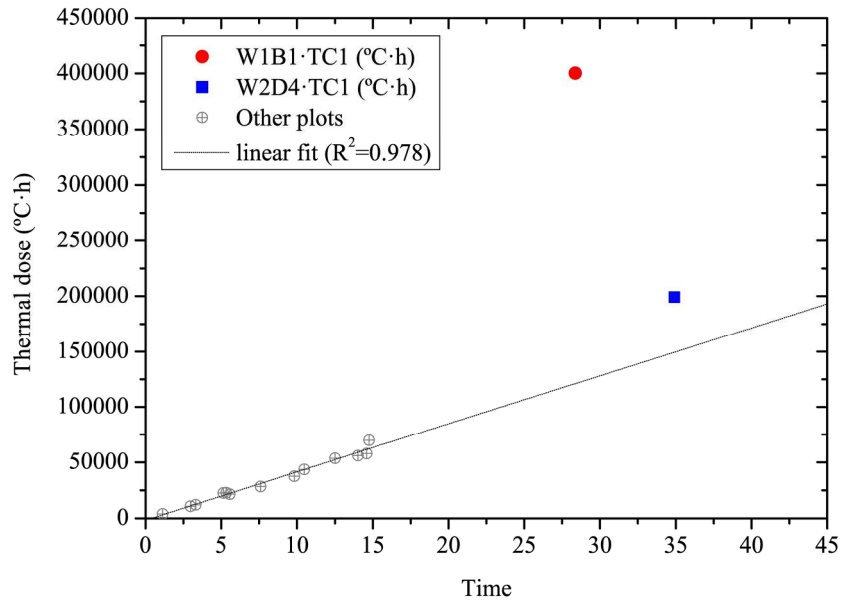


Fig. 6. c) Thermal dose above 60°C, experienced by TC1, TC2 or TC3 thermocouples in all tests.

201x141mm (300 x 300 DPI)

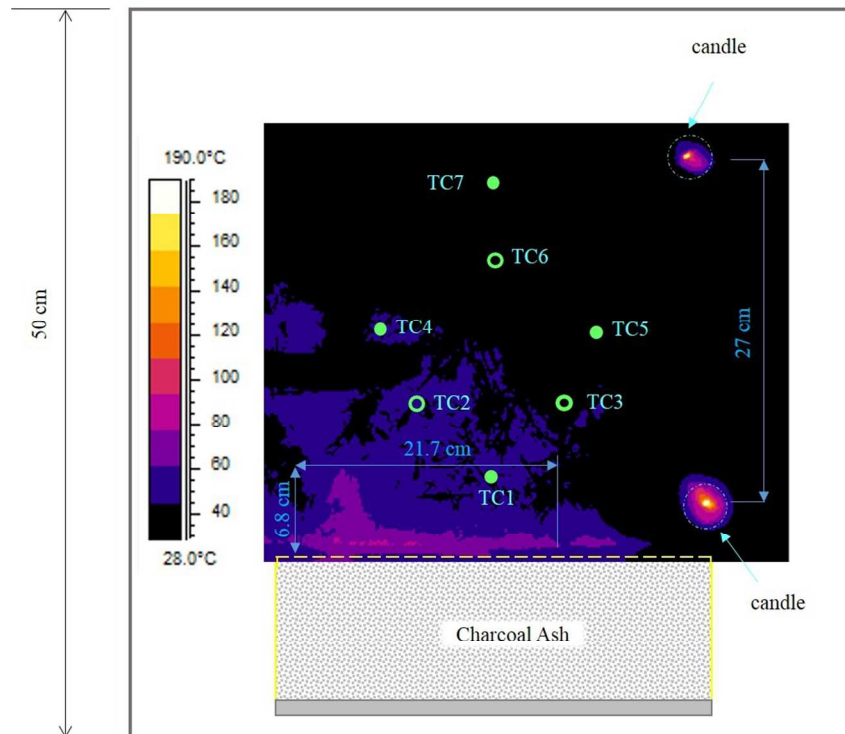


Fig. 7. W1B1 thermal image 24h after ignition, superimposed on a plot and thermocouples layout.

203x151mm (150 x 150 DPI)

Supplementary Information. Relationship between the measured soil moisture with the Hydrosense® probes and the real soil moisture (calculated by natural dry down soil, see Methods section) at each measured soil depth (12 cm, 20 cm).

